

**A MATCHED FIELD PROCESSING FRAMEWORK FOR COHERENT DETECTION OVER LOCAL AND REGIONAL NETWORKS**

Tormod Kværna<sup>1</sup>, David B. Harris<sup>2</sup>, Steven J. Gibbons<sup>1</sup>, and Douglas A. Dodge<sup>3</sup>

NORSAR<sup>1</sup>, Deschutes Signal Processing, LLC<sup>2</sup>, and Lawrence Livermore National Laboratory<sup>3</sup>

Sponsored by the Air Force Research Laboratory and the National Nuclear Security Administration

Contract Nos. FA9453-10-C-0209<sup>1,2</sup> and LL10-BAA10-20-NDD03<sup>3</sup>  
Proposal No. BAA10-20

**ABSTRACT**

The objective of this one-year feasibility study has been to develop a data-adaptive matched field procedure to detect coherently and incoherently across networks of stations at local and regional distances. The detector extends the single-phase matched field processing approach to detection using the entire waveform. We base the procedure upon a narrowband signal representation that exposes invariant spatial and temporal correlation structure of network signals from repeating sources. Wideband multichannel correlators and subspace detectors are both realizations of the resulting detector representation class, of which the matched field detector is an end member. The matched field detector is referred to as an incoherent detector (spatially coherent over a receiver aperture, but temporally incoherent due to the incoherent summation over the narrow frequency bands) and is optimal for sources displaying significant variation in the source time function from event to event. The framework is designed to adapt to the statistics of source time histories for any given target and employs an exponential age-weighting approach to effectively monitor evolving sources, such as open-cast mines.

For a given source of interest, an initial detector is formed. If only a single observation is available, the detector can be either a rank-1 coherent detector (a correlator) or an incoherent detector. If multiple observations are available, an event ensemble can be formed, allowing higher rank subspace detectors. As each subsequent similar signal is detected, a new covariance matrix is formed where the contributions from the waveforms of the existing members of the event ensemble and the newly detected signal are weighted according to processing parameters selected to control the adaptation properties of the detector. The nature of the new detector is determined by the eigenspectrum of the resulting covariance matrix. A covariance matrix with the eigenspectrum heavily concentrated in a single eigenvalue indicates that the phase structures of template components in all frequency bands are locked together and a frequency-coherent processor (correlation detector) is formed. If the energy in the eigenspectrum is dispersed over many eigenvalues, then the emerging processor is a higher-rank subspace projection operator. The rank of the detector is determined by an energy capture criterion.

We have evaluated the framework on datasets in the European Arctic, exploiting extensive existing Ground Truth information, and the Korean Peninsula, where repeating sources have been identified using diverse array processing techniques on the KSRS array. For munitions demolitions at Hukkakero in Finland, observed on the ARCES array, the incoherent detector adapts to a rank-2 subspace detector, reflecting the low variability of signals recorded from this site. A presumed open-cast quarry in South Korea, observed on KSRS, does not produce low-rank detectors and this may be the result of both source variability and low signal SNR. The performance of this detector starts off poorer than that of a single-template waveform correlation detector, missing several events detected by the correlator. As the detector captures more events and adapts to the evolving structure of the wavefield, more events are detected and the correlator is ultimately outperformed. We also examine the 2007 Odaesan earthquake sequence in South Korea for which a higher-rank subspace detector, comprising several of the larger events, detects several events missed by waveform correlators using single events as templates. This demonstrates the subspace detector's ability to represent a greater diversity of source mechanisms and/or an increased geographical footprint. The performance of the incoherent (matched field) detector increases dramatically as the number of available sensors increases. We demonstrate the applicability of matched field and subspace detectors to far larger receiver apertures over which conventional waveform coherence does not apply.

### **OBJECTIVES**

The objective of this one-year feasibility study has been to develop a data-adaptive matched field procedure to detect coherently and incoherently across networks of stations at local and regional distances:

- The detector has extended the existing matched field processing approach, which classifies events on the basis of observations of first-arriving P-waves, to detection using the entire waveform.
- The framework is based upon a narrowband signal representation that exposes invariant spatial and temporal correlation structure of network signals from repeating sources, even in the presence of source-time history variation. It was anticipated that familiar waveform correlation detectors and alternative temporally or spatially incoherent detectors would emerge as special cases of the proposed architecture.
- The specific form of the detector that emerges depends upon the details of correlation structure present in the signal data. The architecture was tested initially against events on the Kola Peninsula, for which good Ground Truth information is available and where signals from repeating sources are observed by network stations and arrays at distances of interest.

Once the basic detection algorithm had been developed and tested, a previously developed autonomous calibration framework was adapted to drive the detector. The new detector replaced the correlation and subspace detectors currently employed in that framework. As the framework operates and collects events from sources of repeating seismicity, the general network covariance is estimated and used to update individual detectors to match the observed correlation characteristics of signals they are designed to detect. As more events are detected, the covariance estimates are updated and used to adapt detectors to be more finely tuned to their targets. The completed framework has been applied to the Korean Peninsula.

### **RESEARCH ACCOMPLISHED**

#### *Introduction*

Empirical Matched Field Processing (EMFP: Harris and Kvarna, 2010) is a method for identifying signals recorded over seismic arrays and networks from repeating sources. Classical f-k analysis assumes a plane-wavefront arriving over a receiver aperture which is small relative to the source-to-receiver distance, and compares the spectral covariance matrix evaluated for an incoming seismic phase with so-called steering vectors which encode the time-delays (phase differences) between the different sensors for a hypothetical incoming wavefront from a given direction. Classical f-k analysis fails when the match between expected and observed phase differences is poor, usually due to scattering and refraction of the seismic waves on structures close to the array.

In EMPF, rather than specifying theoretical steering vectors, we calculate source-specific empirical steering vectors: the eigenvectors of the spectral covariance matrices evaluated on arrivals known to come from the source-region of interest. These steering vectors encode observed phase-shifts and, if required, amplitude differences between the different sensors from actual arrivals from the source under observations, and so already account for the perturbations from the theoretical plane-wavefront which confound classical f-k analysis. In this way, they resemble the multi-channel waveform correlation detectors (e.g. Gibbons and Ringdal, 2006) which assume nothing about the shape of the waveforms recorded and simply exploit the fact that signals on a given sensor configuration act as a "seismic fingerprint" of events within a very limited geographical footprint of the master event. Without the limitation of adherence to the plane wavefront specification, we can exploit far wider receiver apertures than those capable of supporting classical f-k analysis.

EMFP differs from the waveform correlators in that it is a narrowband method and so, in principle, should be less susceptible to differences in the source-time function. Waveform correlation often performs poorly for sources with highly variable source-time functions (such as ripple-fired mining blasts) and EMFP is expected to work better for such sources given that the narrowband covariance matrices characterize the spatial structure of the wavefield on the

receiver network (which is relatively consistent from event to event) rather than the temporal structure (which is specific to a given source-time function). Harris and Kväerna (2010) demonstrated that EMFP using only a short data segment surrounding the initial P-wave arrival attributed seismic signals to the correct source for over 98% of events from a group of mines with a spatial separation far less than the theoretical resolution capability of the array (hence the term "superresolution"). The single-phase matched field statistic for a given template was also demonstrated to be a viable detection statistic (e.g. Ringdal et al., 2010) which motivates the extension of the EMFP approach to one which characterizes the full waveform and not just a short transient.

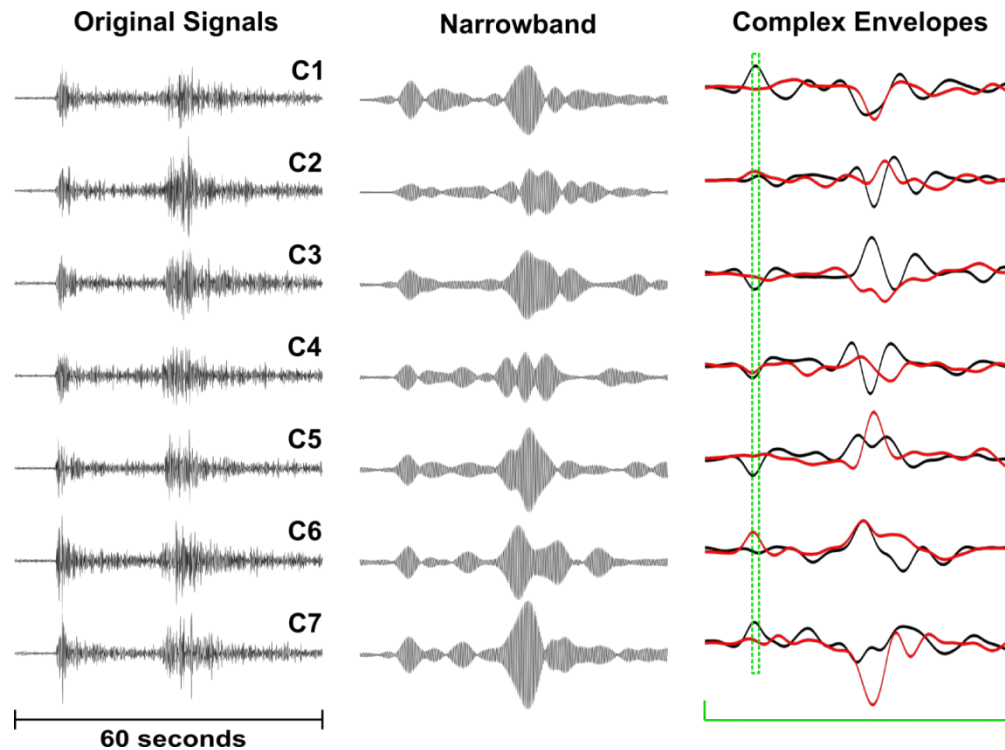


**Figure 1. Complex envelopes obtained by filtering the array waveforms into one particular narrow frequency band. Left, the original signals. Center, the waveforms filtered into a band 0.3125 Hz wide. Right, the corresponding complex envelopes after demodulation to remove the high-frequency carrier. The real part of the envelope is shown in black and the imaginary part is shown in red. The matched field template used for classification in our last contract used only a single sample of the complex envelope around P<sub>n</sub> as indicated by the dashed green rectangle. The detection framework we developed as part of this contract uses the entire waveform, indicated by the green bracket.**

The raw waveforms on the various sensors of the array (left panel of Figure 1) are decomposed with a bank of  $N$  filters resulting in  $N$  complex signals, one for each narrowband component. The narrowband signal (displayed for a single band in the center panel of Figure 1) can be represented by a complex envelope (right hand panel of Figure 1) which varies slowly with time and will capture changes in the relatively slowly varying details of the spatial structure of the signal. As different branches of the wavefield reach different sensors, this alters the phase relationships between the different sensors such that the covariance matrix which characterizes the spatial structure of the wavefield over the sensor aperture at a given time can be constructed from the complex envelopes. A spatial covariance matrix for the entire wavetrain can be obtained from complex vectors comprising discretizations of envelopes which, due to the extreme narrowband nature of the decomposition, can be decimated heavily. Over a population of signals from events at any given source, there may be high correlation between the different frequency bands (which will be the case when the source is highly repeating) or there may be very little correlation between frequency bands (which will be the case when the time-source function varies greatly). The eigenstructure

of the ensemble covariance matrix, evaluated from a large number of events from the source region, should reveal the nature of the source. In a perfectly coherent case (perfectly repeating waveforms) the energy in the eigenspectrum of the ensemble covariance matrix should be concentrated in a single eigenvalue. In the incoherent case, the number of non-zero eigenvalues should be equal to the number of frequency bands.

### *Detection Framework*

In the simpler approach developed for the single phase EMFP detector, a template component was extracted as the principal eigenvector of the covariance matrix for each frequency band and no attempt was made to link templates across frequency bands. In the scheme described here, the covariance matrix incorporates all frequency bands. An eigendecomposition indicating a single non-zero eigenvalue dictates that the template comprise a single eigenvector: a frequency-coherent or correlation detector. An eigenspectrum dispersed over many eigenvalues results in a higher rank subspace detector (Harris 2006a, 2006b) and an appropriate dimension,  $d$ , for the detector must be set by reordering the resulting eigenvalues and selecting the number  $d$  such that the sum of the greatest  $d$  eigenvalues exceeds a specified fraction of the sum of all the eigenvalues. For any given data window to be tested for the presence of a signal, narrowband decomposition is performed prior to the calculation of the complex envelopes as illustrated in Figure 1 and the projection of the resulting data vector into the template subspace is calculated. If only a single event is available with which to characterize a source region, we have the choice of having a frequency-coherent detector (the correlator) or, by forcing independence between frequency bands, an incoherent (matched field) detector.

The purpose of the framework described here is that the detector should be able to evolve according to the nature of the source being observed. If we start with a single event, we can run either a frequency-coherent or incoherent detector. If and when detections occur that can, with confidence, be ascribed to the same source, we can then construct an ensemble covariance matrix and we can determine the rank of the optimal detector according to the eigenstructure of the new covariance matrix. In many situations, e.g., open-cast mines, it may be anticipated that many events will accumulate rapidly (possibly up to several per day). In such cases, it is also likely that the similarity between the signals from two events will decrease as the time between events increases (the Greens function of the source will change as further excavation is carried out). For this reason, we employ an exponential age-weighting algorithm such that the contribution that any one event makes to the ensemble covariance matrix will diminish with time.

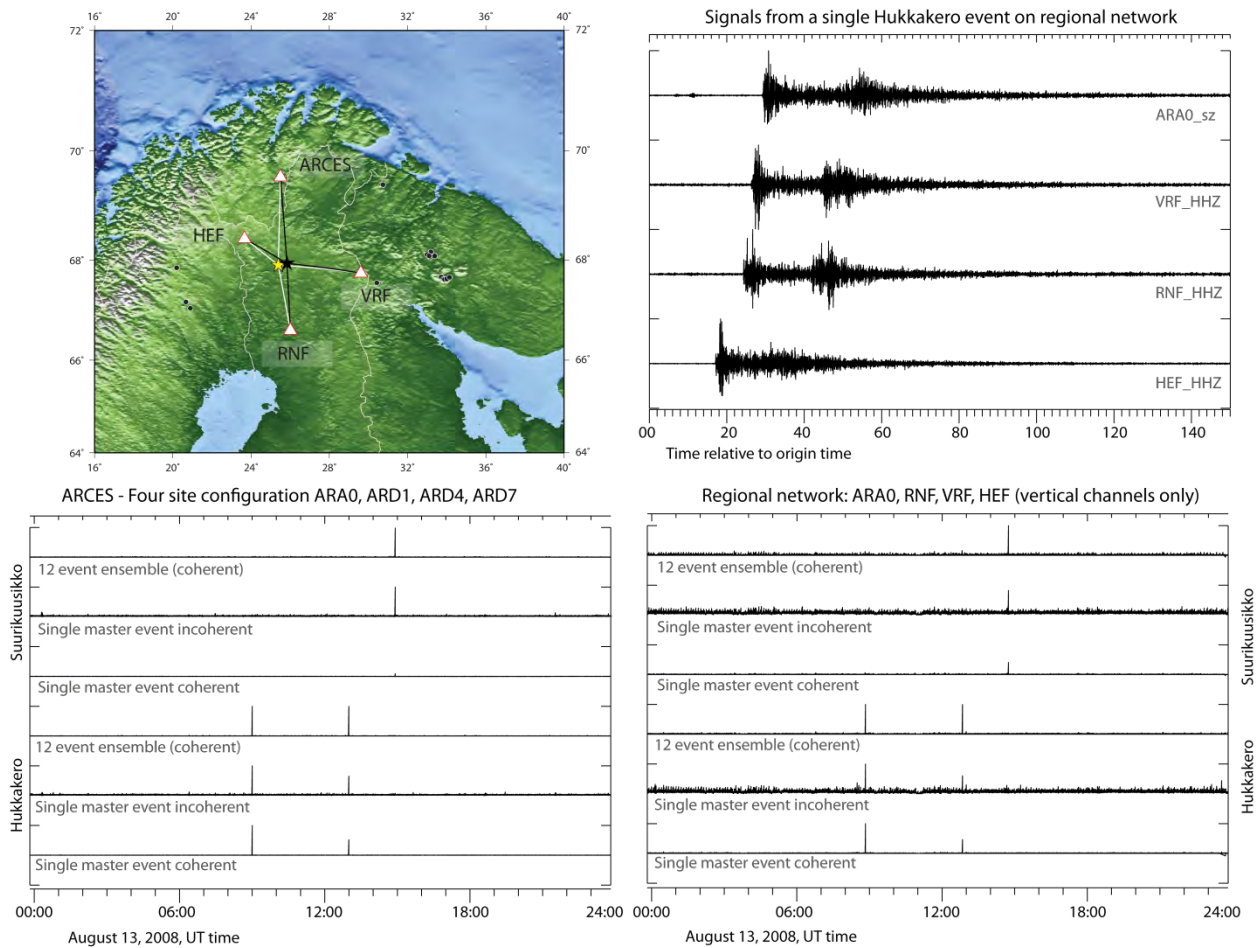
### *Evaluation in the European Arctic*

Figure 2 displays the locations of two sites separated by a little over 10 km in northern Finland. One is a military site at Hukkakero which has been the location of munitions demolition events for at least 20 years. The events have a yield of ~20,000 kg TNT equivalent, all take place within an aperture of ~300 meters, and produce highly repeatable waveforms. The second site is an open-cast gold mine at Suurikuusikko which has been in operation since 2006. The waveform similarity between Suurikuusikko events is also reasonably high (a multi-channel cross-correlation detector on the ARCES array using the algorithm of Gibbons and Ringdal, 2006, has detected many hundreds of events since June 2006 with apparently very few false alarms) although less so than for the Hukkakero shots. Both sites were monitored using two 4-channel sensor networks: a 4-element subset of the short-period vertical channels of the ARCES array (maximum separation ~3 km) and a 4 site virtual network comprising one ARCES channel and the vertical channels of three Finnish network stations.

For both sites, three detectors were run for both sensor networks. The first was a frequency-coherent detector using a single event (a correlation detector in practice). The second was a single event matched field detector with incoherence between frequency bands forced. The third was a matched field detector based on 12 template events with an enforced energy capture of 0.70; for both sites, this resulted in a rank-2 detector.

If we consider first the lowermost trace of the panels, we see two peaks: one at 09:00 UT and one at 13:00 UT. These both correspond to Hukkakero explosions. Although both peaks constitute clear detections, the first peak is significantly greater than the second, indicating greater similarity between the arbitrarily chosen master event and the first event. In contrast, the peaks for the two events are of about the same height for the rank-2 detector. For the Suurikuusikko example, we see also that the ensemble detector detects the single event that day with a higher value

of the normalized detection statistic than for the single event correlator. It is of course possible that other randomly chosen single event correlators would have resulted in an even higher value of the detection statistic. An important point demonstrated here is that the method works both on the small aperture array and the large aperture network. The noise level associated with the incoherent matched field detector appears to be much higher for the sparse network than for the array. This may be due to waveform dissimilarity, but may also be due to other complications of inhomogeneity across the network (e.g. interpolation of waveforms into a uniform sampling rate). In an associated experiment, the ensemble covariance matrix for the Hukkakero explosions was updated with other Hukkakero events from the archives. The detector converged to a rank-2 subspace detector.

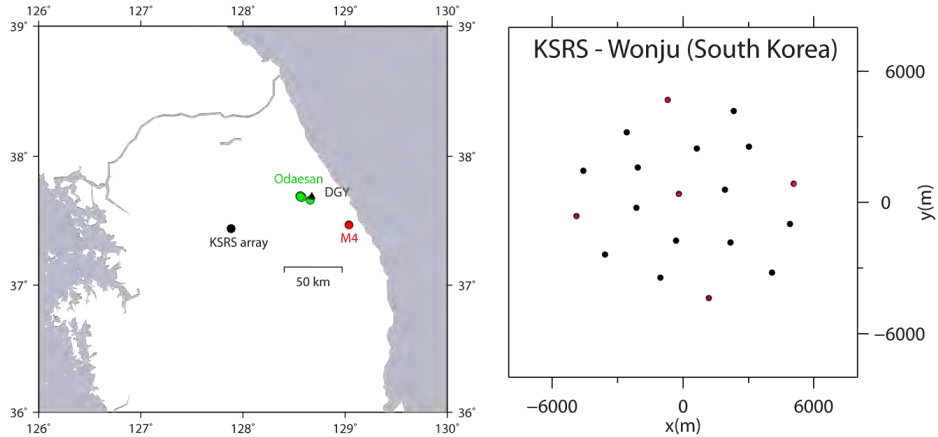


**Figure 2. Performance of incoherent and coherent detectors on two seismic sources in the European Arctic. (Top left) Map showing location of the Suurikuusikko gold mine (yellow) and Hukkakero military explosion site (black) relative to the ARCES array and 3 stations in Finland. (Top right) Signals from a Hukkakero blast recorded on the sparse network. (Lower left) Matched field detection statistics for templates as indicated on a 4-site subset of ARCES. (Lower right) As for the panel on the left but for the 4-site sparse network.**

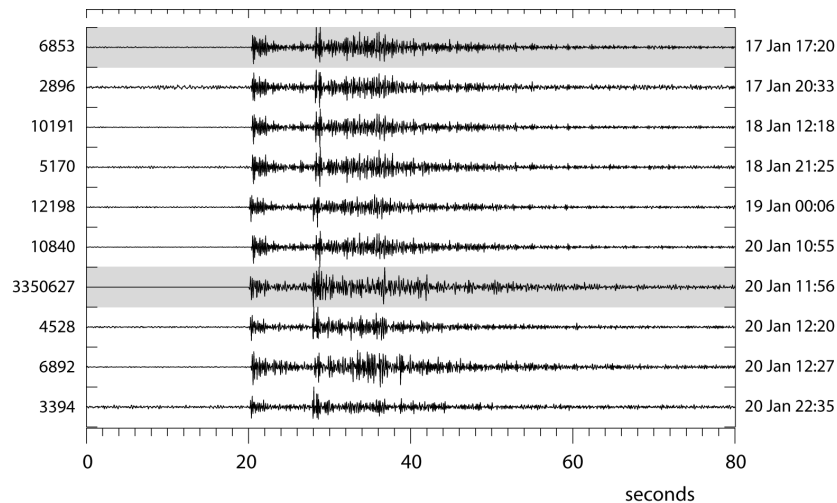
*Application to the Korean Peninsula*

A large database of repeating seismic sources on the Korean Peninsula was obtained using only data from the KSRS teleseismic array in a 3 stage procedure. Firstly, high frequency regional phases were detected using the incoherent spectrogram beamforming method of Gibbons et al. (2008) with slowness estimates being made using coherent f-k

analysis in the 2-4 Hz frequency band. Secondly, events were formed by associating regional P and S phases with manual retiming of arrivals. Thirdly, clusters were sought using full array waveform correlation and the post-processing algorithm of Gibbons and Ringdal (2006). Two of the sites identified are displayed in Figure 3. The first group of events are earthquakes in the so-called Odaesan sequence (Kim and Park, 2010) consisting of a magnitude 4.8 earthquake on January 20, 2007, and numerous smaller events in the days following January 17, 2007. The second group comprises presumed quarry blasts at a site labelled M4, of which there are several events each week, all of magnitude less than 2.



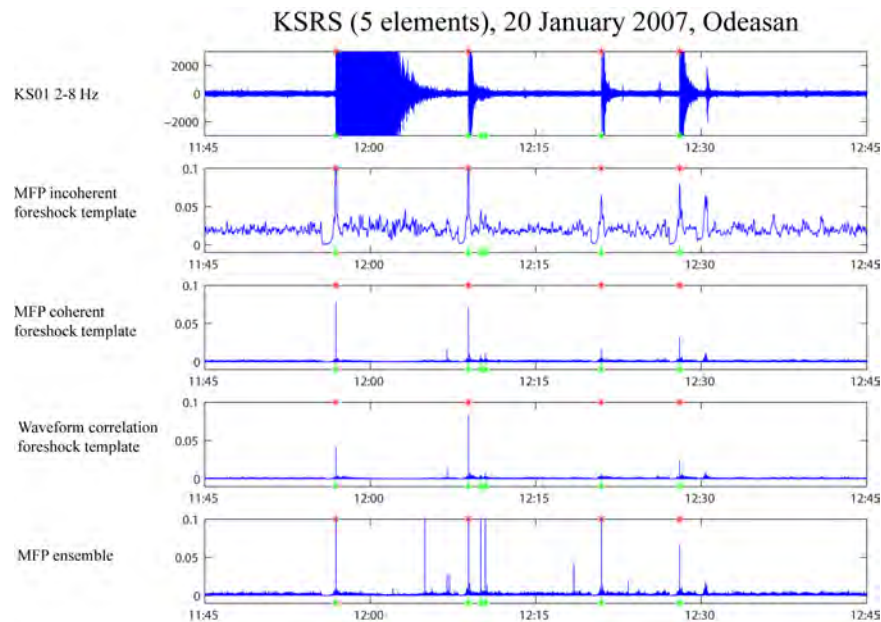
**Figure 3. (Left) Map showing the location of the KRSRS array in South Korea, the Odaesan earthquakes (green filled circles), the M4 mine (red filled circle) and the DGY three-component station operated by the Korea Meteorological Administration (KMA). (Right) Sensor distribution of the 19-element KRSRS array in South Korea. Red symbols show the location of the 5 sensors used for initial testing of the MF detector.**



**Figure 4. Panel of 10 events from the Odaesan earthquake sequence recorded at the KS01\_SHZ sensor of the KRSRS array. The data are bandpass filtered between 2 and 8 Hz. The highlighted upper trace shows the foreshock used for single-event incoherent and coherent MF detection processing, as well as for detection using array-based waveform correlation. The highlighted trace no. 7 from top shows a recording of the main mb 4.8 event. The ensemble of all 10 events was also used for coherent MF detection processing. The event origin times are given to right of each trace, and the corresponding maximum amplitudes are given to the left.**

Figure 4 displays waveforms on KRSRS from 10 of the largest events in the Odaesan sequence (note the large contrast in amplitudes with over 3 orders of magnitude separating largest from smallest events).

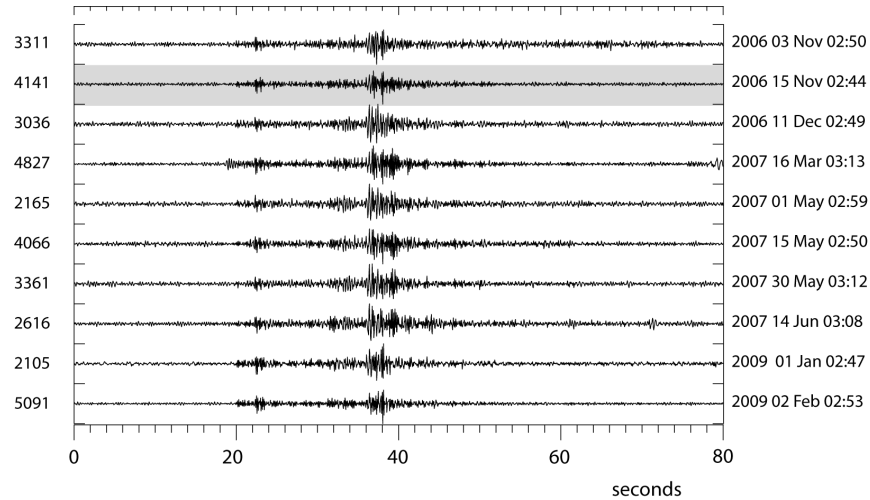
Figure 5 displays the results of attempting to detect events using various pattern detectors in a one hour long segment on January 20, 2007, containing the largest event. Using the waveforms from the first event displayed in Figure 4, three different detectors were set up: a waveform correlation detector in the Gibbons and Ringdal (2006) formulation, a frequency-coherent (rank-1) matched field detector, and an incoherent matched field detector. A fourth detector, a rank-3 subspace detector based upon all ten of the events displayed in Figure 4, is displayed in the lowermost trace. The key results here are that the incoherent single-event detector appears to identify all of the events detected by the 19-channel correlator featuring the first event, and that the higher rank matched field detector detects several events which are barely detected by the single event detector. This indicates that the broader geographical footprint and/or wider range of source mechanisms is better represented by the higher rank detector.



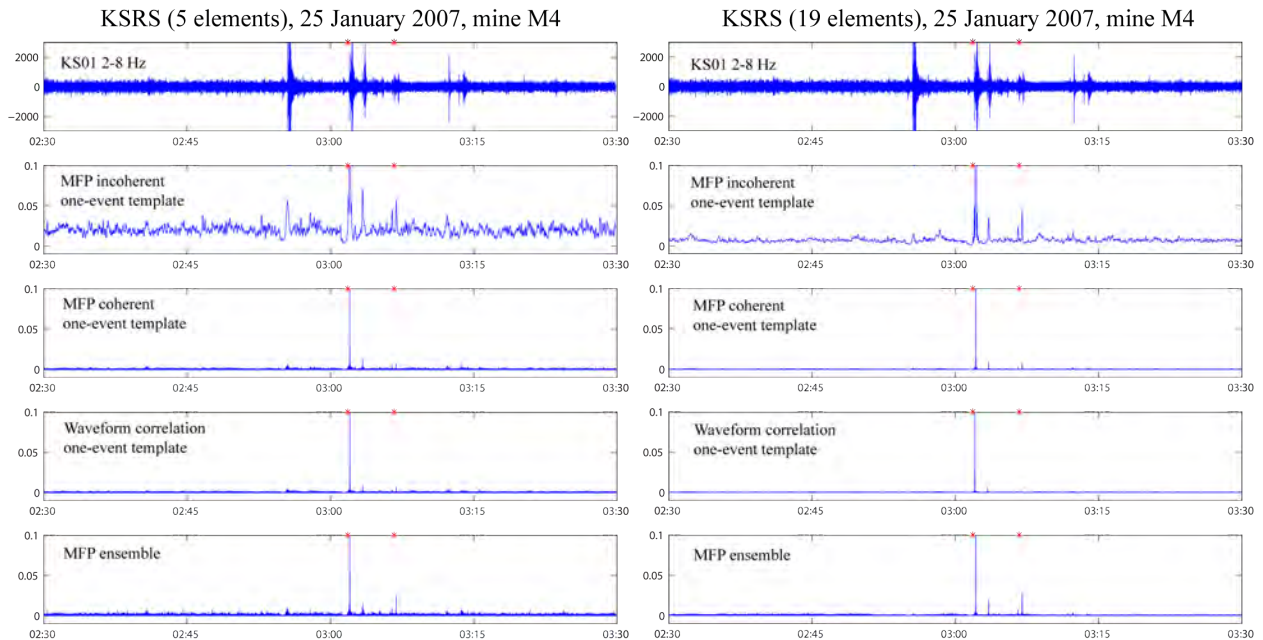
**Figure 5. Detector processing results using the five KSRS SHZ sensors KS01, KS08, KS11, KS14 and KS17 for a one-hour time interval around the largest event of the Odaesan earthquake sequence (Kim and Park, 2010). The upper trace shows recordings at one sensor of the KSRS array (KS01) filtered in the passband 2-8 Hz. Traces 2-4 from top show different detector outputs as indicated where a 60 s data segment of the event seen around 17:20 is used as the template. Trace no. 5 shows the detector output using the ensemble of the ten Odaesan events displayed in Figure 4. The red stars indicate event candidates found by waveform correlation utilizing all 19 sensors of the KSRS array, and green symbols indicate events reported by Kim and Park (2010). To get an impression of the background noise variability, the maximum vertical scale of the detector outputs is set to 0.1. As a result, the largest detection “peaks” are clipped.**

Figure 6 displays waveforms from ten events deemed to belong to the cluster denoted M4; a presumed mine. The performance of a number of pattern detectors is displayed in Figure 7 for a one hour period. The most striking result is the improvement to the performance of the incoherent single-event resulting from the increase in the number of sensors from 5 to 19. As for the Hukkakero explosions, we ran the adaptive process whereby new events were added progressively to the ensemble covariance matrix. Whereas the Hukkakero detector converged to a rank-2 detector, the M4 mine detector failed to converge to a low rank. To maintain energy capture at the 0.75 level, a rank-8 detector was necessary. The reason for this may be a combination of diversity of the sources and low signal-to-noise ratio (SNR), particularly apparent in Figure 8. (It should be stressed that the 10 events displayed in Figure 6 used to form the initial ensemble covariance matrix all result from the spectrogram beamforming power detector process and therefore necessarily have a relatively high SNR.) Figure 9 compares the performance of the single event correlation detector with the exponential age-weighting adaptive matched field detector. It is clear that, at the start, the correlator detects a number of events missed by the matched field detector and, at the end, the matched field detector picks up events missed by the correlator. However, it is important to note that the correlator template did

not undergo any modification in this time period and that renewal of the waveform template may have improved the performance substantially. This is however indicative that the adaptive nature of the procedure described here makes the method appropriate for classification of quarry blasts over long periods of time over which the wavefield evolves.



**Figure 6.** Panel of 10 events from the from the M4 mine recorded at the KS01\_SHZ sensor of the KSRS array. The data are bandpass filtered between 2 and 8 Hz. The highlighted trace no. 2 shows the event used for single-event incoherent and coherent MF detection processing, as well as for detection using array-based waveform correlation. The ensemble of all 10 events was also used for coherent MF detection processing. The event origin times are given to right of each trace, and the corresponding maximum amplitudes are given to the left.



**Figure 7.** Analogous to Figure 5 except for the time of the data segment and the fact that the ensemble is constructed from the M4 mine events displayed in Figure 6. The left panel uses the 5 element subset of KSRS and the right panel uses the full array.

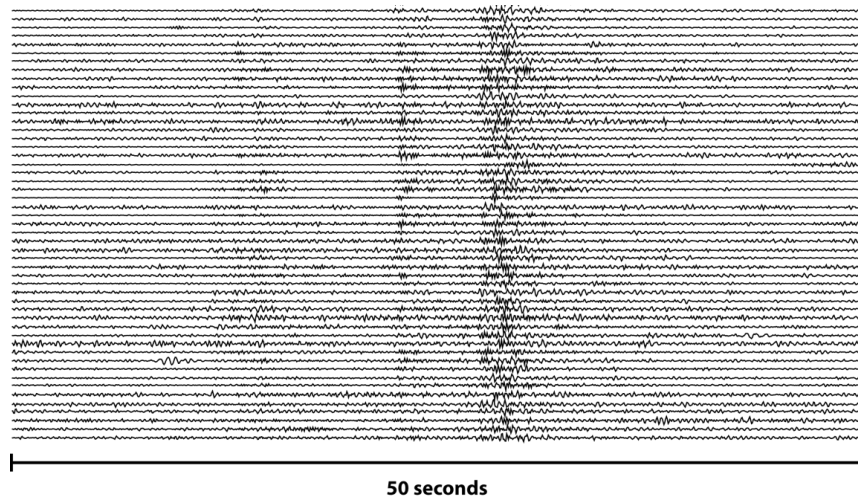


Figure 8. Some of the 70 M4 detections that were used in the template adaptation process. Note that very weak P phase(s), Sn and Lg are present. One channel of the KSRS array is shown filtered into the detection band (2-8 Hz).

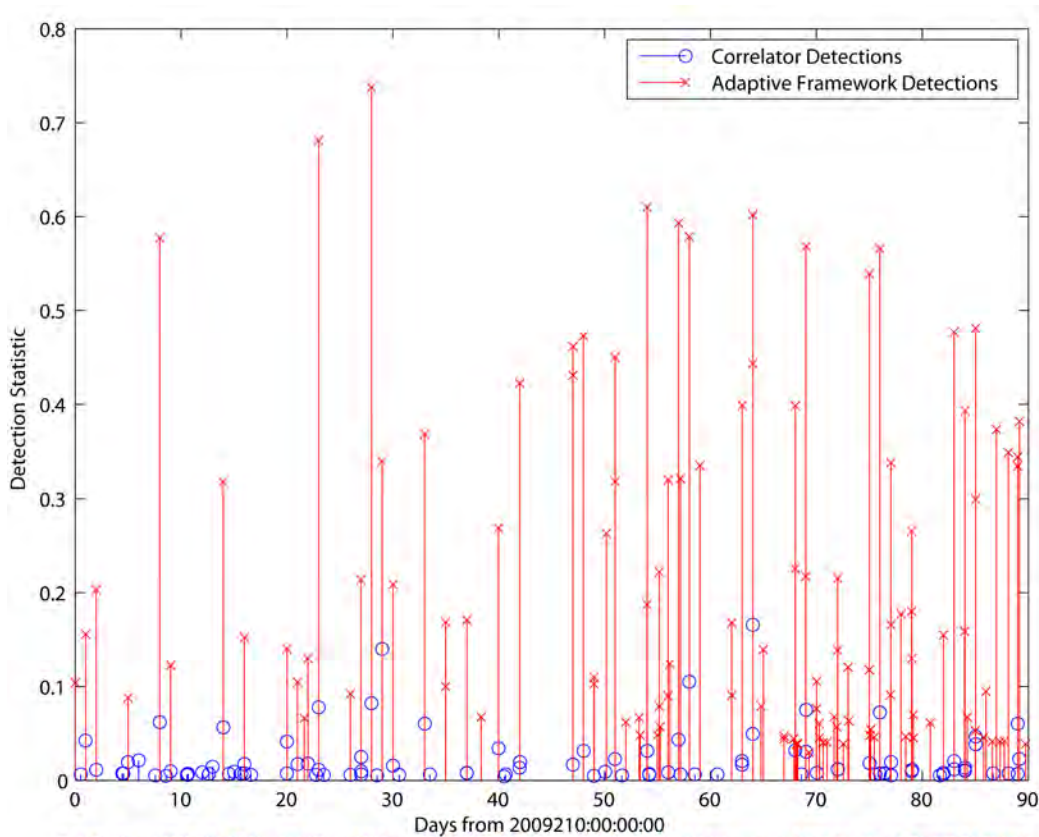


Figure 9. Comparison of correlator detections (blue) of M4 events and adaptive framework detections (red). At first the adaptive framework detector misses many of the lower SNR events found by the fixed correlator (up through about 17 days). But as the detector burns in it captures larger numbers of the events defined by the correlator (and even some missed by the correlator).

## CONCLUSIONS AND RECOMMENDATIONS

In this project we have demonstrated that it is possible to generalize the single-phase matched field processing template developed in a previous contract to a template constructed from an entire seismogram. The general template is multichannel and multidimensional, with the number of dimensions being controlled by the number of narrow bands used to decompose the wideband master event waveform. This template can be used as a basis for a detection algorithm implemented in a subspace detector framework. Furthermore, the framework can represent correlation detectors and the incoherent (narrowband) matched field detectors and gradations between the two. We have shown that detectors in the framework can be made to adapt, as new event waveforms become available, through a subspace update mechanism. A detector that begins as a matched field detector will adapt to resemble a correlation detector, if the source produces highly repeatable waveforms. We have demonstrated this form of adaptation with a highly repeatable source in Fennoscandia, and we have also demonstrated somewhat different adaptive behavior that improves detection performance with a mining explosion source in the Korean peninsula. We have demonstrated that the performance of the matched field detector can improve dramatically as the number of available sensors increases, and have demonstrated the applicability of matched field and subspace detectors to far larger apertures over which conventional notions of waveform coherence do not apply.

## REFERENCES

- Gibbons, S.J. & Ringdal, F. (2006): The detection of low magnitude seismic events using array-based waveform correlation. *Geophys. J. Int.* 165: 149–166.
- Gibbons, S. J., Ringdal, F., and Kvaerna, T. (2008): Detection and characterization of seismic phases using continuous spectral estimation on incoherent and partially coherent arrays, *Geophys. J. Int.* 172: pp. 405–421.
- Harris, D. B. (2006a). Subspace Detectors: Theory. Lawrence Livermore National Laboratory Report UCRL-TR-222758.
- Harris, D. B. (2006b): Subspace Detectors: Efficient Implementation. Lawrence Livermore National Laboratory Report UCRL-TR-223177.
- Harris, D. B. and Kvaerna, T. (2010): Superresolution with seismic arrays using empirical matched field processing, *Geophys. J. Int.* 182: 1455–1477.
- Kim, K.-H. and Park, Y. (2010): The 20 January 2007 ML 4.8 Odaesan Earthquake and its Implications for Regional Tectonics in Korea, *Bull. Seism. Soc. Am.*, 100: pp. 1395–1405.
- Ringdal, F., Harris, D. B., Kvaerna, T., and Gibbons, S. J. (2010): Expanding coherent array processing to larger array apertures using empirical matched field processing, in *Proceedings of the 2010 Monitoring Research Review: Ground-Based Nuclear Monitoring Technologies*, LA-UR-10-05578, Vol. 1, pp. 318-327.